

Knotting Within the Gluing Bifurcation

Philip Holmes

Robert Ghrist

Departments of Theoretical and Applied
Mechanics and Mathematics and
Center for Applied Mathematics

Center for Applied Mathematics

Cornell University
Ithaca, NY 14853 USA

Abstract

After a brief review of the uses of *knots* and *templates* in bifurcation theory for three dimensional flows, we begin an examination of the class of homoclinic bifurcations known as *gluing bifurcations* from a knot-theoretic point of view. We present a topological classification of the periodic orbits which appear in the gluing bifurcations associated with a *saddle* fixed point: that is, an equilibrium point having all real eigenvalues in the linearization. For this classification, the global twisting of the flow about the orbits is of fundamental importance. We use the associated template to show the predominance of *torus knots* among the orbits created in these bifurcations.

1 Knots, templates, and the topology of bifurcations

In a three dimensional flow, a periodic orbit defines a knot, by the uniqueness of solutions of ODE's. Adopting this viewpoint enables us to import a vast body of results and techniques from theoretical knot and link theory to understand the topology of periodic orbits. This in turn lends itself naturally to the bifurcation problem for a parametrized family of flows: given a class of orbits, from what bifurcations did they arise, and in what order? Many problems in nonlinear oscillations are amenable to such an analysis; in particular, many "chaotic" systems exhibit infinitely many knot types (e.g., the Lorenz system [BW83a] and the suspended Smale horseshoe map [HW85, GH93]), providing a rich topological structure for analysis.

The knot-theoretic approach to bifurcations is very natural. For example, consider a saddle-node bifurcation of periodic orbits. Intuitively, one can think of the two orbits growing closer and closer together until they coalesce at the bifurcation point and then disappear. From the uniqueness of solutions, it then follows that these orbits have the same *knot type* (that is, as embeddings of S^1 , they are *ambient isotopic*). Furthermore, they must be *linked* with all other coexisting orbits in precisely the same manner, again, in order to maintain uniqueness of solutions. Therefore, knowledge of topological data immediately yields bifurcation invariants. Other local bifurcations have analogous topological interpretations, e.g., a period multiplying bifurcation corresponds to a *cabling* of the knot [Hol86].

The strategy for examining systems via knot-theoretical techniques is as follows: given a three dimensional flow, "embed" it in a parametrized family for which certain elements have well-understood behavior, e.g., a certain class of knots is unique, or perhaps non-existent. Then, varying parameters back to the original system, one traces bifurcations

back, keeping track of knotting and linking to “match up” with orbits in the original system. This approach has unearthed surprising behavior in a family of Hénon maps [HW85, Hol86, Hol89]. Other systems which have been examined include the (geometric) Lorenz system [BW83a] and the perturbed pendulum (Josephson junction) equation [Hol87]. In general, these methods are also of use in understanding the ordering of bifurcations in the creation of horseshoes [HW85] in chaotic systems. Knot and braid theory has also found its way into the analysis of experimental time-series data [MSN⁺91], and, in connection with numerical simulation, in bifurcation studies of periodically forced oscillators [MT93a, MT93b]. Here we will focus on results for a specific class of bifurcations. Our aim is to completely describe the knot and link types of all periodic orbits created in the global “gluing bifurcations” which occur near a degenerate homoclinic orbit in a dissipative three dimensional flow. We then envisage the use of continuation methods to follow these orbits far (in parameter space) from their origin and thus reveal global genealogies. Although we will be brief in our review of the necessary theory, the interested reader may consult [GH93] for a thorough introduction. We wish to stress that although the first papers in the subject appeared over ten years ago [BW83a, BW83b], there is a great deal left to be done — the subject is still in its infancy.

In order for such an approach to be useful, however, one must be able to efficiently extract topological information from a system. Thus, we turn to the dimension-reducing tool of Birman and Williams: the *template* [BW83a, BW83b]. For three dimensional flows which satisfy certain conditions, one identifies orbits which have the same future behavior; in effect, one collapses each fiber in a strong stable foliation down to a point. The result projects the three dimensional flow to a *semi-flow* on a *branched two-manifold* which is the template. An example will best serve to illustrate. For the geometric Lorenz system [GW79], collapsing out the strong stable direction yields the template \mathcal{T} pictured in Figure 1:

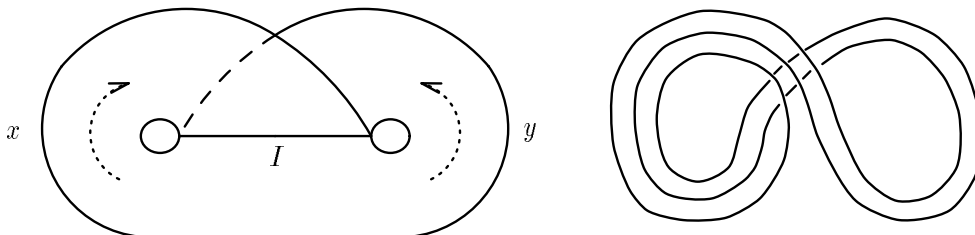


Figure 1: The Lorenz template and a periodic orbit

This is essentially what one sees in numerical experiments on the Lorenz equations: cf. Figure 3 of [Lor63]. There are two *branches*, x and y , which meet at the branchline I . The three dimensional flow is now a two dimensional semi-flow since one cannot “flow backwards” at the branchline. The utility of templates lies in the following theorem [BW83a, BW83b]:

Theorem 1 (the Template Theorem) *Given a flow on a three-manifold having a hyperbolic chain recurrent set, there exists a template such that (with perhaps one or two exceptions) the collapsing map is one-to-one on the union of periodic orbits via an ambient isotopy (i.e., a continuous deformation preserving all knotting and linking information).*

Organizing knots on the template is simplified by the following symbolic tool: given a periodic orbit on \mathcal{T} , we may describe it by a finite word in the symbols x and y by

recording the order in which the orbit travels along the x and y branches. For example, Figure 1 shows the Lorenz template with the periodic orbit $xyxy(=x^2yxy)$ (*Exercise: is this knotted?*). Of course, cyclic permutations (shifts) of a word do not change the orbit: $x^2yxy = xyxyx$.

We may therefore by Theorem 1 describe all orbits in our original system symbolically. Upon noting that the branchline is a natural choice for a Poincaré section, we may extract the (one dimensional) first return map, which for the Lorenz system is an expanding map of the interval with a single discontinuity (see [GH83] §2.3, §6.4).

In summary, we may use the structure inherent in the template to examine the topology of the orbits. We may then turn to the one dimensional return map and invoke the tools of *kneading theory* and *symbolic dynamics* to relate various knots to bifurcations in the system [GH93, HW85]. Such an analysis is typically a blend of topological visualization and symbolic manipulations. As an example, we reprove a proposition from [BW83a] which will be of use in classifying knotted orbits in the gluing bifurcation.

First, we recall the definition of a particular family of knots. A *torus knot* is a knot which can be arranged to fit on the surface of the standardly embedded torus $T^2 = S^1 \times S^1 \subset \mathbf{R}^3$. We say the torus knot is of type (p, q) for $p, q \in \mathbf{Z}$ if it winds around the longitudinal direction p times and around the meridional direction q times. We require p, q be relatively prime and note that, except for the relation $(p, q) \sim (q, p)$, these two integers completely classify and distinguish all torus knots [Rol77]. We note that the family of torus knots is a very restrictive class, of which a great deal is known. Identifying torus knots in flows has been useful in bifurcation analyses [HW85, Hol86].

Consider again the Lorenz template \mathcal{T} and the symbolic description of knots. There are infinitely many (but not all!) knot types coexisting on \mathcal{T} , some of which are torus knots. Consider an *evenly distributed* word in x and y , that is, a word composed of syllables of only the forms xy^k, xy^{k+1} or $x^ky, x^{k+1}y$ (cf. Section 2 below): for example, x^2yxy and xy^3xy^4 are evenly distributed while x^3y^2 and xy^3xy^5 are not. In [BW83a], the following is stated:

Proposition 1 *On \mathcal{T} , an evenly distributed word corresponds to a torus knot.*

Proof: Say the given word has p x 's and q y 's and assume that $p > q$ (If $q > p$, flip \mathcal{T} about the vertical axis and proceed by symmetry). Then, since the word is evenly distributed, there are no consecutive y 's: each loop about the y -branch is immediately followed by a loop about the x -branch. As such, we may fit the orbit within an unbranched subtemplate $\mathcal{S} \subset \mathcal{T}$ and isotope it as per Figure 2. What remains after these visual gymnastics is a ribbon containing the orbit which fits on the torus T^2 such that the orbit winds p times longitudinally and q times meridionally: a (p, q) torus knot. \square

2 The gluing bifurcation

The bifurcation problem has been examined from a knot-theoretic viewpoint so far only in the cases of local bifurcations such as saddle-node and period-multiplying bifurcations [GH93, Hol88]. Global bifurcations are more subtle in that one requires information along an entire trajectory of the flow: e.g., in homoclinic bifurcation theory, one examines orbits

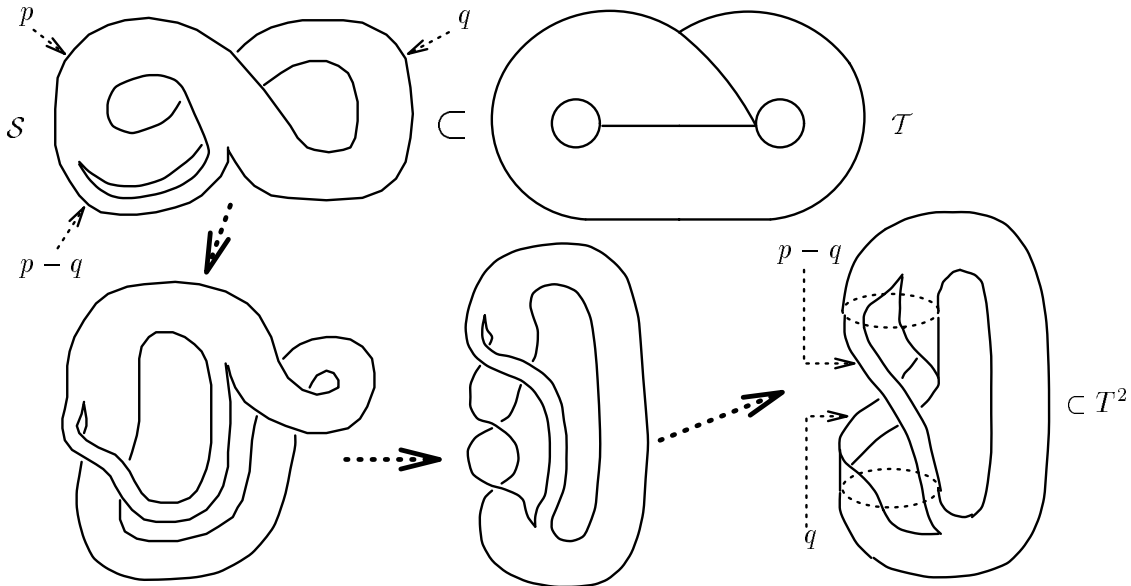


Figure 2: The subtemplate \mathcal{S} fits on T^2 . The letters p, q , and $p - q$ refer to the number of strands on each ribbon.

which bifurcate from a homoclinic connection. Our goal is to introduce the knot-theoretic viewpoint to the study of global bifurcations by means of a simple example of a homoclinic bifurcation: the so-called *gluing bifurcation* [CGT84, GGT88, Gle88].

Consider a system $\dot{x} = f(x)$ (where f is C^1 with uniformly Lipschitz partials) having two orbits, γ_x and γ_y , homoclinic to a hyperbolic fixed point p . For the gluing bifurcation, it is necessary that the unique unstable eigenvalue $\lambda_u (> 0) \in \mathbf{R}$ be *weak* in the sense that $\lambda_u < |\Re \lambda_i|$ for all other stable eigenvalues λ_i ($\Re \lambda_i < 0$). Finally, to permit linearization near p , we require no first-order resonances among the eigenvalues:

$$\Re(\lambda_i) \neq \lambda_u + \Re(\lambda_j) \quad \forall i, j. \quad (1)$$

We will be interested in a neighborhood W of $\Upsilon = \gamma_x \cup \gamma_y$ for C^1 perturbations of such *critical* systems. One describes the periodic orbits emerging in the unfolding of a critical system symbolically, as with orbits on the template. Assuming Υ is bounded away from other fixed points and taking W to be a small neighborhood of Υ , orbits in W cannot “double back” and must follow Υ monotonically. In fact, the weak eigenvalue assumption implies that the flow is contracting and hence that there is an attractor contained in W . Thus, labeling γ_x, γ_y with the letters x, y we can assign to any periodic orbit γ in W a finite acyclic word in x and y given by what order it travels around each loop: this is the orbit’s *signature*. Just as in the case of template orbits, we have a shift equivalence class of words, since beginning at a different point yields a cyclic permutation of the word.

In a gluing bifurcation, it is possible to have periodic orbits with nontrivial words, e.g. x^2yxy . Which words are possible is at the heart of understanding the unfolding. It is a fact stated in [GGT88, Gle88] that any periodic orbit bifurcating from Υ in a critical system has a *rotation compatible* signature. That is, it may be obtained as the symbol sequence of a point $z \in I$ iterated by a rotation map $\rho_\theta : z \mapsto (z + \theta) \bmod 1$ with the partition $I_x = (0, 1 - \theta], I_y = (1 - \theta, 1]$ for some $\theta \in [0, 1)$. Given such a word, the unique θ for that word is called the *rotation number*. Note: to compute the rotation number from a given rotation compatible word, take the number of y ’s and divide by the total

length of the word: e.g., $x^2yxy \Rightarrow \theta = \frac{2}{5}$. In short, we can describe rotation compatible words as precisely the “evenly distributed” words of Proposition 1: we may then define the rotation number uniquely by the above formula.

The main result concerning the gluing bifurcation is the following (see [CGT84, GT88]):

Theorem 2 *For every sufficiently small C^1 perturbation of a critical system there are at most two periodic orbits in a small neighborhood W of Υ . Any periodic orbits which may be present are attracting and have rotation compatible signatures. Finally, if there are two periodic orbits, then their associated rotation numbers are Farey neighbors.*

We recall that two rational numbers $\frac{p}{q}$ and $\frac{p'}{q'}$ are *Farey neighbors* if $|pq' - qp'| = 1$.

The fact that at most two periodic orbits exist follows from the observation that the attractor lies within the closure of the one dimensional unstable manifold $W^u(p)$, of which there are two “sides” (separated by p). Although Theorem 2 severely restricts the number and type of periodic orbits near Υ , there is nevertheless enough latitude within many such systems to allow for bifurcation diagrams with infinitely many curves [GGT84]. In such a contracting system, unlike the expanding Lorenz flow, at most two periodic orbits can coexist, but as parameters vary, we will see that infinitely many periodic orbits (and knot types) may be created and annihilated, depending upon the global structure of the system.

We complete our review by recalling the universal features of the unfolding of a gluing bifurcation [CGT84, Gle88]. Let

$$\dot{x} = f(x; \alpha, \beta) \quad : \quad x \in \mathbf{R}^3; \quad \alpha, \beta \in \mathbf{R} \quad (2)$$

be a continuous two-parameter family of systems for which $f(x, 0, 0)$ is a critical system. Construct a cylindrical ($S^1 \times I$) Poincaré section Σ to the fixed point p (assumed fixed under variation of parameters) transversal to $W_{loc}^s(p)$. The local unstable manifold $W_{loc}^u(p)$ is one dimensional: set up local coordinates about p having $W_{loc}^u(p)$ as the u -axis. At $\alpha = \beta = 0$, the two homoclinic orbits first hit Σ in two points, each with zero u -coordinate. Turning on the bifurcation parameters α, β will send the “first” intersections of $W^u(p)$ with Σ to the points with u -coordinates $\mu(\alpha, \beta), -\nu(\alpha, \beta)$. Assuming these are locally invertible functions, we may choose μ and ν to be the unfolding parameters for the system. Having done this, one can show:

Proposition 2 *For (μ, ν) sufficiently small, the parameter space has the structure appearing in Figure 3, where the notation “ $x : y$ ” denotes coexistence of two orbits. The periodic orbit signatures are completely determined except within the two “wedges” defined to lowest order by*

$$-c_1\nu^\delta < \mu < c_2\nu^\delta; \nu > 0 \quad \quad -c_3\mu^\delta < \nu < c_4\mu^\delta; \mu > 0 \quad (3)$$

where $c_i > 0$ and $\delta > 1$.

It is precisely these undetermined wedges of Proposition 2 which make this bifurcation interesting.

The gluing bifurcation takes its name from the fact that, as one varies parameters from the third quadrant to the first quadrant through the origin, the two “simple” coexistent periodic orbits x and y are glued together in the double homoclinic connection Υ which then breaks to form a *single* periodic orbit xy .

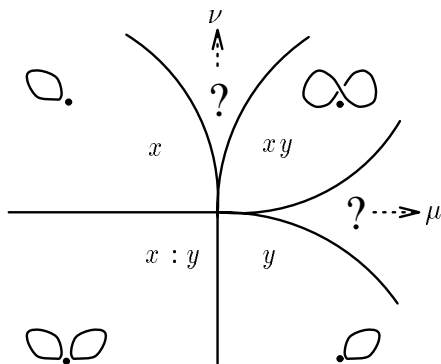


Figure 3: The parameter plane unfolding

3 Topological classification of the real saddle

We will be interested in examining a three dimensional critical system having a (*real*) *saddle* fixed point p : i.e., all the eigenvalues of the linearization are real. This implies that there is no “spiraling” of $W^u(p)$ into p . As such, there are two distinct topological configurations depending upon which sides of $W_{loc}^s(p)$ the the homoclinic orbits reenter: these are the *figure-of-eight* and the *butterfly*, given in Figure 4. Our goal is to provide a

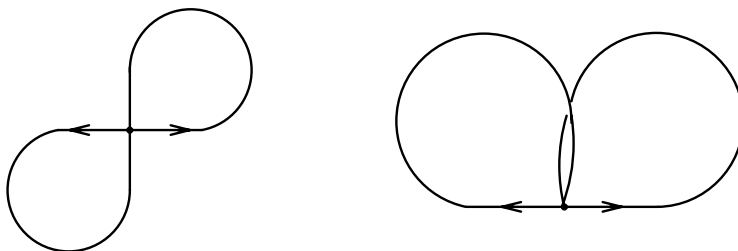


Figure 4: The figure-of-eight and butterfly configurations

topological classification of the periodic orbits which may appear in these configurations, with emphasis on the latter. For these systems, we assume the existence of a strong stable foliation (reported in [Gle88] to be a generic condition in these cases) and proceed to collapse such foliations out, leaving a template. The associated semiflows on such templates are *contracting*, whereas *expanding* templates have been the norm in the literature. More precisely, we have a two-parameter (μ, ν) family of templates, each of which holds, by Theorem 2, at most two closed orbits.

It is noted that the templates we construct for these systems must be embedded in \mathbf{R}^3 . Thus, we must take into account the “twist” of the flow around the homoclinic connections, which will correspond to certain branches of the template being likewise twisted. At this time, we ignore more exotic, knotted embeddings of the template branches.

3.1 Classification of the butterfly

The templates associated with the butterfly configuration are similar to their expanding cousin, the Lorenz template. Temporarily disregarding extraneous twisting, there are

three cases to consider: *untwisted*, *singly-twisted*, and *doubly-twisted*.¹ These appear in Figure 5 in this order. Taking the branchline as a Poincaré section, the first return

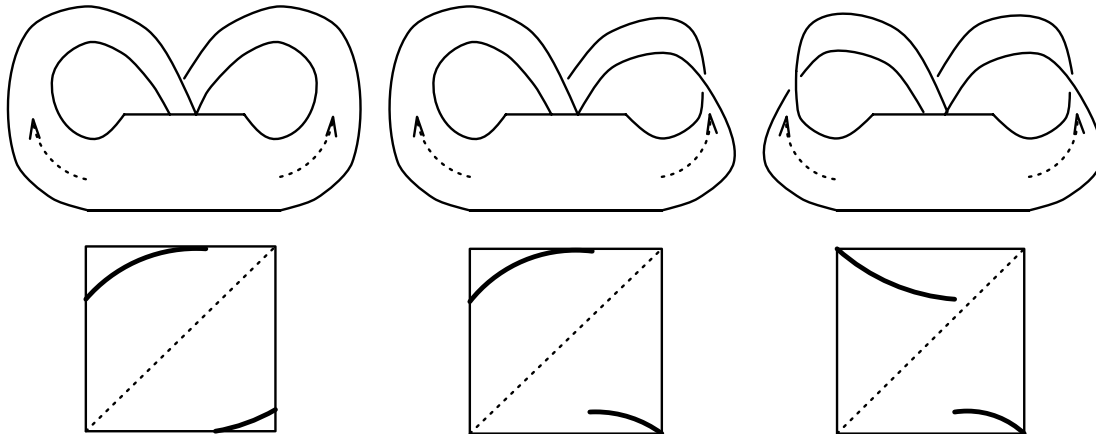


Figure 5: The three templates (above) with induced maps (below)

map is discontinuous and one dimensional. By performing a local analysis at the fixed point, and assuming an affine global return map along the branches (cf. the derivation in [GPTT, Gle88]), the return map in a sufficiently small neighborhood of the degenerate homoclinic loop ($\mu = \nu = 0$) is equivalent to

$$f_{\mu, \nu} : \xi \mapsto \begin{cases} \mu - a|\xi|^\delta & : \xi \leq 0 \\ -\nu + b\xi^\delta & : \xi > 0 \end{cases}, \quad (4)$$

where $\delta > 1$, μ and ν are the unfolding parameters as above, and the signs of a, b depend upon the orientability of the x, y branches respectively (negative if twisted, positive if untwisted). We note that δ is the ratio of the weakest stable eigenvalue to the unstable eigenvalue, and $\delta > 1$ corresponds to our assumption that the latter be weak (see §2). Representatives of these maps appear below their template counterparts in Figure 5. In contrast to the Lorenz first return map, these are *contracting* maps of the interval with a single discontinuity.

3.1.1 Case (1) : untwisted ($a, b > 0$)

It is stated in [Gle88, GT85] that for $\mu, \nu > 0$ this system has at most one periodic orbit, based on the theory of circle maps (one views the map as a monotone injective map of the circle with a single discontinuity). The structure in other regions of the parameter plane is trivial and covered by the general theory [Gle88]. It is possible to find periodic orbits with nontrivial knot types; however, since the signature of any orbit must be a rotation compatible word, and since these are precisely the words which are evenly distributed, we may call upon Proposition 1. Note that although the *dynamics* of this butterfly system differ greatly from that of the Lorenz, the associated templates are isotopic (we can deform one to the other). Therefore, we have:

¹The expanding counterparts to these three systems appear in [ABS82] as *oriented*, *semioriented*, and *nonoriented* respectively.

Corollary 1 *Any periodic orbit appearing in the unfolding of an untwisted butterfly saddle is a torus knot. If the rotation number of the signature is $\theta = \frac{p}{q+p}$, then the corresponding knot type is (p, q) .*

For example, the orbit with signature x^2yxy is a $(2, 3)$ torus knot: a *trefoil*. It is very significant that only torus knots appear: in the expanding case, one has a *much* wider array of knot types [BW83a]. Corollary 1 is reminiscent of the Morgan-Wada theorem, which states that nonsingular zero-entropy flows in S^3 yield only torus knots, with perhaps additional cablings and connected sums thereof [Mor78, Wad89]. Though this theorem does not apply to the systems we are examining, the weak unstable eigenvalue assumption nevertheless yields a “tame” family of flows, whose periodic orbits we expect to be related to simple classes of knots. And again, we stress that embedding this template in a more complicated fashion may not yield torus knots: see the remarks below.

The unfolding of the bifurcation in this case has been stated in [GPTT, PTT87, TS87]. We recall the unfolding diagram along with the stable orbits² of (4) numerically computed along a slice of constant $\nu > 0$ in Figure 6. Note the existence of “tongues” of orbits of fixed rotation number and that the rotation number is a continuous monotonic function of each parameter. Those (measure zero) regions for which the rotation number is irrational correspond to the existence of a nonperiodic attractor about which the unstable manifold winds irrationally [Zak93].

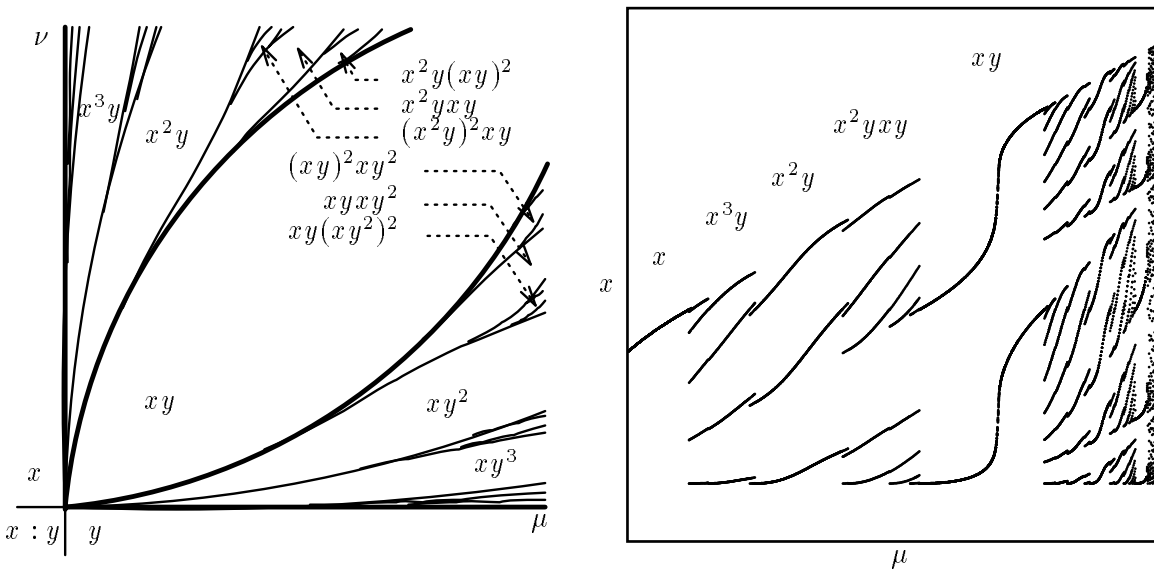


Figure 6: The parameter plane unfolding and a bifurcation diagram: case (1)

We now consider the impact of introducing τ_x (even) positive half-twists along the x branch. Corollary 1 is no longer applicable; however, we note that in the isotopy moves from the proof of Proposition 1, the x -branch may be fixed. As such, we may let τ_x be nonzero and perform the same moves without any interference on the part of the τ_x half-twists. In this case, since τ_x is even (i.e., there are $\frac{1}{2}\tau_x$ full twists) we then get a $(p, q + \frac{1}{2}p\tau_x)$ torus knot. Similarly, a related set of isotopy moves may be performed which

²Note there exists a unique orbit for each μ , cf. Figure 10. We have labeled only those lying in the largest tongues.

will present the (p, q) torus knot as a braid on q strands, this time leaving the right y -branch fixed. As before, if $\tau_x = 0$, we may insert τ_y (even) twists to obtain a $(p + \frac{1}{2}q\tau_y, q)$ torus knot.

We cannot, however, obtain a torus knot when τ_x and τ_y are simultaneously non-zero and even: no set of isotopy moves exists which leaves both branches fixed. While we are unable to identify the knot types of orbits for arbitrary τ_x, τ_y in terms of well-known families, we can arrange the knot into a braid on p -strands. Let it be an exercise for the reader to isotope the appropriate subtemplate to the braided form presented in Figure 7:

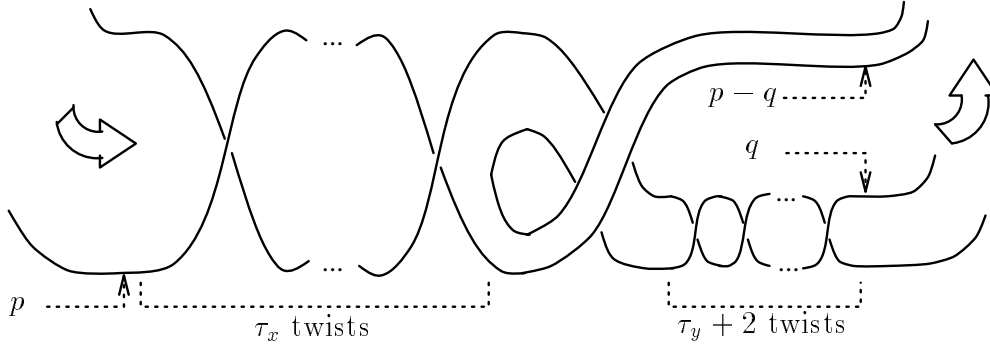


Figure 7: Braided subtemplate

This presentation defines an element γ of the p -strand *braid group* B_p [Bir75]: that is, the orbit is presented so that it travels monotonically around a *braid axis* (coming out of the page above Figure 7) p -times. The generators of B_p , $\{\sigma_i : i = 1 \dots p - 1\}$, each represent the crossing of the i^{th} strand over the $(i+1)^{\text{st}}$: in this way, we can express the periodic orbit in terms of the σ_i and hence represent symbolically the crossing information. Though they are algebraic entities, the geometric interpretations of the braid groups permit numerous applications to the study of periodic orbits [Boy, MT93a]. We use the following notation: let Δ_k^m denote m half-twists on the first k strands, and let χ_k^m represent the crossing of the first m strands over the next k strands (see Figure 8). Then, from Figure 7, we may write γ as

$$\gamma = \Delta_p^{\tau_x} \chi_q^{p-q} \Delta_q^{\tau_y+2}. \quad (5)$$

Now, noting that

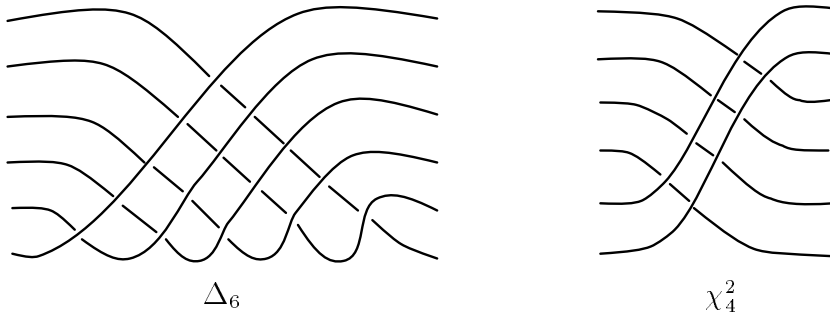


Figure 8: Twists and crossovers

$$\Delta_k^1 = \prod_{i=1}^{k-1} \left(\prod_{j=1}^{k-i} \sigma_j \right), \quad \chi_k^m = \prod_{i=1}^m \left(\prod_{j=1}^k \sigma_{m-i+j} \right), \quad (6)$$

we may explicitly write out the element of B_p defined by the periodic orbit γ for arbitrary τ_x, τ_y . From the braid presentation in Figure 7, it may be shown that for $\tau_x = \tau_y$ positive and even, the orbit lies on $T^2 \# T^2$, the standardly embedded surface of genus two.

In addition, when τ_x, τ_y are positive and even this presentation of the periodic orbit as a positive braid on p strands permits computation of the genus g of the knot by the formula [BW83a, GH93]

$$g = \frac{c - p + 1}{2}, \quad (7)$$

where c is the number of crossings in the braid presentation. This number may be directly counted:

$$c(\Delta_k^1) = \sum_{i=1}^{k-1} i = \frac{1}{2}k(k-1), \quad c(\chi_k^m) = mk. \quad (8)$$

This implies

$$c(\gamma) = c(\Delta_p^{\tau_x}) + c(\chi_q^{p-q}) + c(\Delta_q^{\tau_y+2}) \quad (9)$$

$$= \frac{1}{2}(\tau_x p(p-1)) + (p-q)q + \frac{1}{2}((\tau_y+2)q(q-1)). \quad (10)$$

And thus, the genus of an arbitrary periodic orbit is

$$g = \frac{1}{2} \left(\frac{\tau_x}{2} p(p-1) + \frac{\tau_y}{2} q(q-1) + (p-1)(q-1) \right). \quad (11)$$

Note that when $\tau_x = \tau_y = 0$, this reduces to $g = \frac{1}{2}(p-1)(q-1)$, the genus of the (p, q) torus knot [Rol77], as expected.

The braid presentation of Figure 7 also yields another invariant: the *braid index*, or, the minimal number of strands on which a knot may be presented as a braid. Again, assuming $p > q$ and τ_x, τ_y positive, if $\tau_x \geq 2$ it follows by a theorem of Franks and Williams [FW87] that the braid index is precisely p (see [GH93, HW85] for applications of the braid index and genus in distinguishing periodic orbits).

3.1.2 Case (2) : singly-twisted ($a > 0 > b$)

In this case where global (odd) twisting occurs along one branch of the template, the existence and uniqueness results available from rotation map theory are no longer available; however, we may still apply Theorem 2 to limit the possible behavior. Assume without loss that the y -branch is twisted (i.e., $a > 0 > b$ in (4)). The other case is equivalent via symmetry. The class of maps (4) are difficult to analyze in general, but appealing to the template semiflow will provide a geometric argument for the following:

Proposition 3 *If the y -branch of the butterfly template has a half-twist (case (2)) then all periodic orbits appearing on it must have signature x or $x^k y$ ($k \geq 0$). The same holds reversing x and y .*

Proof: We begin by showing that no two consecutive y 's can occur. Although this can be proved directly from the nature of the 1-d map, the following ‘‘template’’ argument will set the tone for subsequent steps. Assume the existence of a closed orbit containing

a pair of points $y_1 \neq y_2$ on the “right half” of the branchline (I_y) which are consecutive with respect to the flow. Flow y_1 forwards on the template, traveling once around the y -branch and connecting to y_2 . Now, flow y_2 forwards until it intersects the branchline again. Since the semiflow is contracting and orientation reversing about the y -branch, y_2 must flow again around the y branch to a point $y_3 \in I_y$ which lies *between* y_1 and y_2 : in this interval the orbit is now forever trapped (iterate the preceding argument), implying that the orbit was not periodic as assumed.

Now, we show that there can be only one y in the entire signature. This time, assume the existence of a closed orbit containing $y_1, y_2 \in I_y$ such that $y_1 < y_2$ with y_2 the first intersection of I_y with the image of y_1 under the semiflow. As before, flow y_1 until it reaches y_2 ; then continue flowing. Eventually, perhaps after traversing the x -branch numerous times, the image of y_2 will intersect I_y at a point y_3 (see Figure 9). Since the y -branch reverses order, $y_3 < y_2$. In addition, since the semiflow is contracting, $y_3 > y_1$: i.e., $y_3 \in (y_1, y_2)$ as before. Iterating the argument gives the next intersection point $y_4 \in (y_3, y_2)$, etc. — the orbit is successively trapped and is consequently nonperiodic. \square

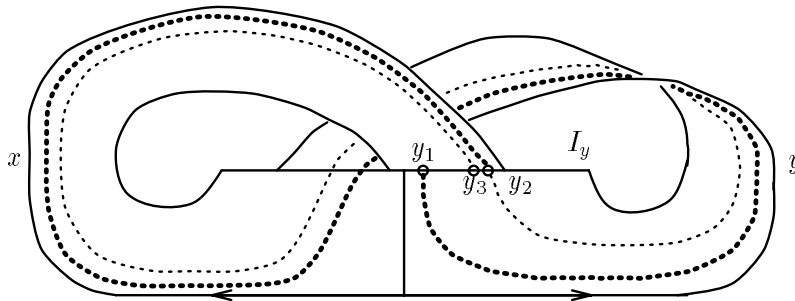


Figure 9: y_3 is “trapped” within (y_1, y_2)

The argument associated with Figure 9 implies the following:

Corollary 2 *All orbits in the unfolding of a singly-twisted butterfly are either periodic, asymptotically periodic, or homoclinic: there is no irrational winding as is possible in the untwisted case.*

Proof: As soon as an orbit itinerary contains two distinct y 's, Figure 9 implies that the orbit is “trapped” and the itinerary is henceforth periodic. Thus, all itineraries are either finite (homoclinic orbit) or eventually periodic. \square

Knowledge of the possible signatures from Proposition 3 then determines the possible knot types. Although Figure 9 is drawn for the case $\tau_x = 0$, Proposition 3 and Corollary 2 are true for any evenly twisted x -branch, embedded in any way (even knotted). The following corollary, however, is specific to $\tau_x = 0$:

Corollary 3 *Any periodic orbit appearing in the unfolding of a singly-twisted butterfly saddle is an unknot.*

Turning now to the unfolding of this bifurcation, we encounter a situation quite different from that of the untwisted case. In this singly-twisted case we cannot relate the first-return maps to rotation maps in order to prove the uniqueness of periodic orbits: in fact, coexistence does occur.

Proposition 4 *The unfolding of the singly-twisted butterfly system is as given in Figure 10.³ In particular, there exist open regions in the first quadrant of the parameter plane for which the periodic orbits $x^k y$ and $x^{k+1} y$ coexist, for each $k \geq 0$.*

As in Figure 6, Figure 10 also contains numerically computed stable orbits⁴ along a slice of constant $\nu > 0$. *Exercise:* what is the linking number of the coexisting orbits?

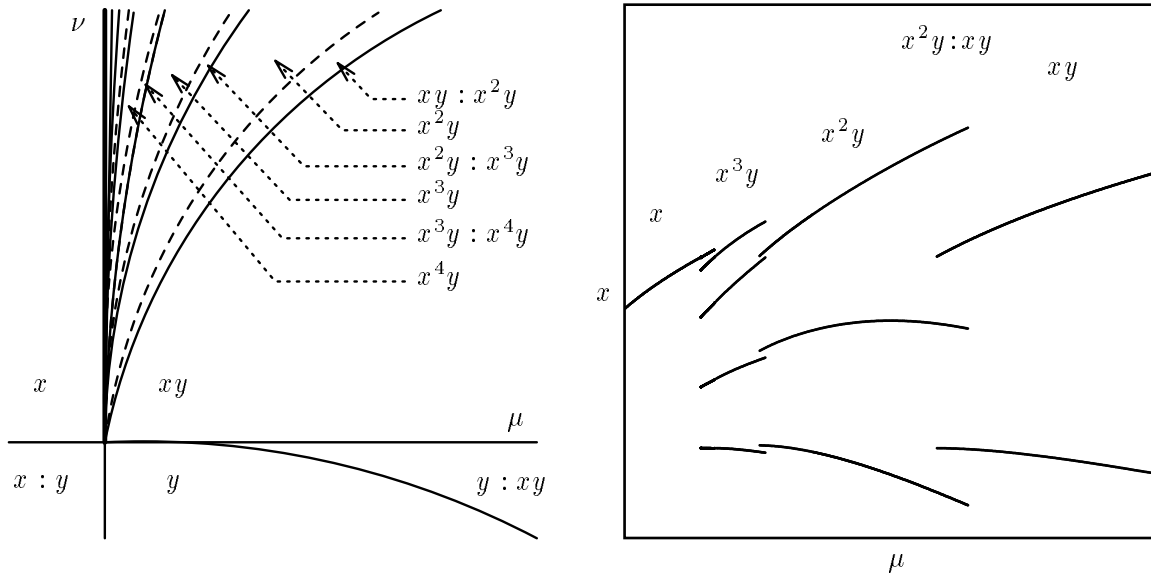


Figure 10: The parameter plane unfolding and a bifurcation diagram : case (2)

The proof of Proposition 4 is based on the examination of homoclinic connections and their subsequent breakings. Given a homoclinic connection in the flow, one may pass to the template and look at the corresponding homoclinic connection there.⁵ Upon breaking a connection by (say) fixing ν and perturbing μ , the ω -limit sets of the two branches of the unstable manifold $W^u(p)$ are determined by the restricted topology of the branched two-manifold. Within the template, it is observed that the stable manifold $W^s(p)$ “surrounds” the ω -limit set of one branch of $W^u(p)$ on one side of the bifurcation. Hence, the ω -limit set of the second branch of $W^u(p)$ cannot coincide with that of the first: i.e., there is a coexistence of periodic orbits on one side of the bifurcation. Knowing the signatures of the possible orbits from Proposition 3, the Farey neighbor property of Theorem 2 then implies that for $x^k y$ and $x^j y$ to coexist, $|k - j| = 1$. Without plunging into the details, we remark that these facts completely determine the behavior associated with single homoclinic connections within this system. Having done this, the unfolding diagram is a simple matter of placing the bifurcations in the unique order which fills in the gaps in Figure 3 of Proposition 2. \square

Considering now more complicated embeddings of this template, let there be τ_x, τ_y half-twists in the x and y branches respectively, with τ_x even, τ_y odd. Since all periodic

³Cf. Figure 3 of [TS87], where there is a mislabeling in the upper right corner.

⁴Note the Farey neighboring orbits which coexist in the overlapping regions of the tongues.

⁵The astute reader will note that a homoclinic connection is sent to a point by the template collapsing map; thus, the corresponding homoclinic connection is technically not defined. We circumvent this technicality by considering the homoclinic orbit as the limit of a sequence of periodic orbits of increasing period, each of which has a well-defined template counterpart which approaches a homoclinic connection for the semiflow.

orbits (besides x) are of the form $x^k y$, there is a unique y -strand and thus τ_y does not influence the knot type. So, taking the k strands wrapped about the untwisted x -branch and inserting $\frac{1}{2}\tau_x$ full twists yields a braid on k strands which naturally fits onto a torus: these are $(k, \frac{1}{2}k\tau_x + 1)$ torus knots. It is worth noting that one cannot obtain arbitrary types of torus knot, as is possible in Case (1). For example, the torus knots of types $(3,5)$, $(4,7)$, $(5,7)$, $(3,8)$,... are all incompatible with the above formula, and therefore nonexistent, irrespective of global twisting.

3.1.3 Case (3) : doubly-twisted ($a, b < 0$)

This is the simplest case. Recall, the first step in the proof of Proposition 3: when the y -branch is twisted, a y must be followed by an x . This applies equally well to the doubly-twisted case, for both x and y branches. Thus, there are no orbits having signatures containing x^2 or y^2 .

Corollary 4 *Any periodic orbit appearing in the unfolding of a double-twisted butterfly saddle has signature x , y , or xy : all of which are unknots.*

As this map may be interpreted as a monotone injective map of the circle with a single discontinuity, we may again prove that there is a unique periodic orbit for $\mu, \nu > 0$. The corresponding unfolding is not difficult to determine, nor is it as interesting as the previous two cases. The simplicity of these periodic orbits prevents any knots from forming, even under arbitrary amounts of additional (odd) twisting in the branches.

3.2 Classification of the figure-of-eight

The associated figure-of-eight template is not branched, but is a standard compact two-manifold whose form mirrors its namesake: there are two ribbons which meet together in a neighborhood of the fixed point. Along each branch of the template, there may be an arbitrary number of half-twists in the ribbons, depending upon the global twisting in the flow about $W^u(p)$. This yields the template given in Figure 11. Let $\tau_x, \tau_y \in \mathbb{Z}$ be the

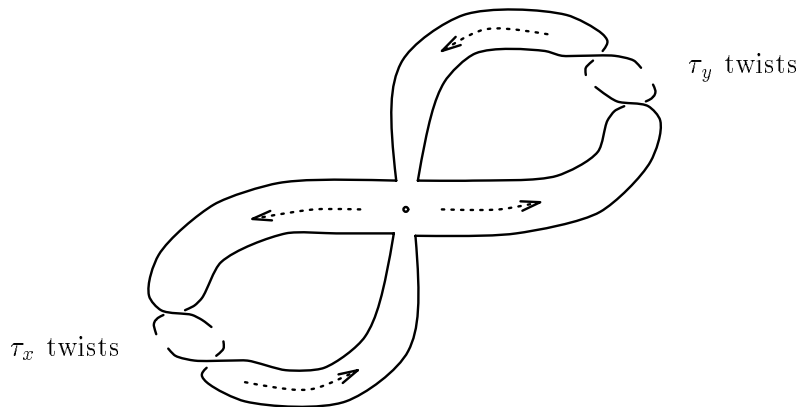


Figure 11: The figure-of-eight template

number of half-twists in the template x and y branches. As in the butterfly configuration,

the unfolding of the gluing bifurcation for this case will break down into untwisted, singly-twisted, and doubly-twisted cases, depending on τ_x and τ_y , each *mod* 2. Imitating the proof of Proposition 3, though, one can show:

Proposition 5 *In a figure-of-eight configuration, any periodic orbit resulting from a gluing bifurcation must have signature xy , $x(yx)^k$, or $y(xy)^k$ for some $k \geq 0$.*

In the untwisted and singly-twisted cases, only the simplest orbits ($x^k y, xy^k; k \leq 2$) can appear. The unfoldings are likewise simple and left to the reader (see [BGKM91] §4.5.2 for help in the untwisted case). In the doubly-twisted case, one can use an argument similar to that of Proposition 4 to obtain the bifurcation diagram given as Figure 12. In

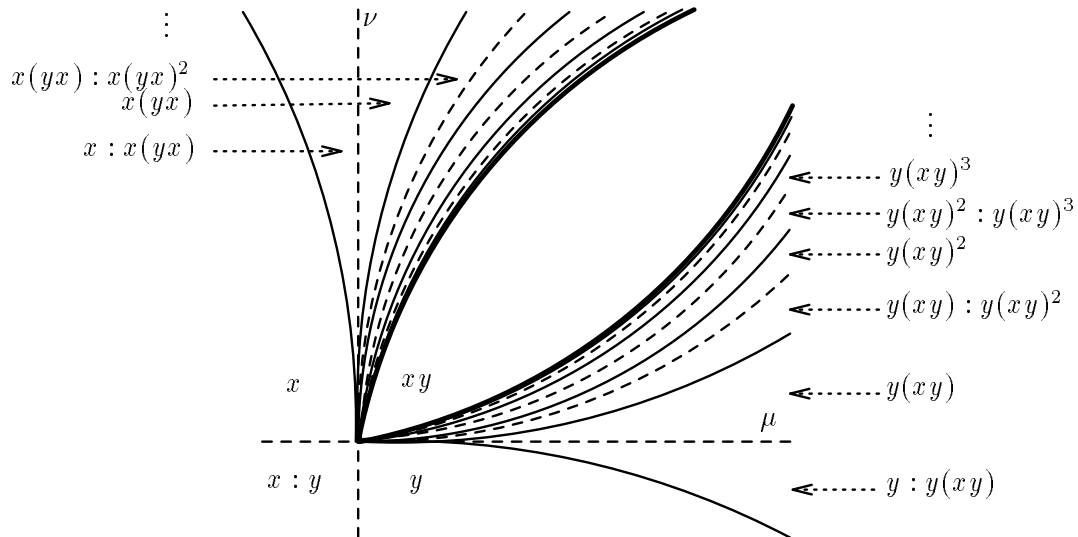


Figure 12: The parameter plane unfolding : doubly-twisted figure-of-eight

the more general cases where τ_x, τ_y are arbitrary, any periodic orbits in the untwisted or singly-twisted configurations are either unknots or simple two-strand torus knots. For the doubly-twisted case as pictured in Figure 12, the reader may verify that, for $k > 0$, the orbit $y(xy)^k$ has braid index k if $\tau_y = 1$ (resp. $k + 1$ if $\tau_y \geq 3$) and genus

$$g = \frac{1}{4}k[(\tau_x + \tau_y)k - \tau_x + \tau_y - 2]. \quad (12)$$

4 Conclusion

This exploration of knotting and linking phenomena present in the gluing bifurcation is the first step of the general strategy mentioned in §1. A thorough understanding of the topology and unfoldings associated with gluing bifurcation will then permit connections to more complex systems via parametrized families. The subsequent application of topological bifurcation invariants (knot types, linking information) may then lend insight into the bifurcation sequences giving rise to highly complicated systems. For example, if the eigenvalue ratio δ is regarded as a third bifurcation parameter in the unfolding, then as δ decreases through one and the saddle point's unstable eigenvalue begins to dominate, the butterfly template acquires the expansive property of the "standard" Lorenz system

and infinitely many periodic orbits and knot types appear. From classifications such as Corollary 1, we can say that, among these, only certain torus knots and unknots can be followed from $\delta > 1$.

We stress that, in establishing global genealogies of orbits in rather general flows, we cannot rely on special braid structures which exist in forced oscillators, for example, but must allow for gross distortions. Thus, the symbolic descriptions in terms of the letters $\{x, y\}$, which distinguish orbits as long as they remain within the small neighborhood W , are no longer invariants. Here, the knotting and linking data is crucial: to this end, the template construction has been, and continues to be, a useful tool.

In addition to this overt goal, it is worthwhile to examine the gluing bifurcation for its own sake. As the periodic orbits associated with the bifurcations are attracting, they may be readily observed in experimental data. Indeed, gluing bifurcations have been identified in various physical models, e.g. [MP87, BGKM91].

For the gluing bifurcations associated with a real saddle point, we have noted the predominance of unknots and torus knots among the orbits: this is particularly encouraging as such orbits then have numerous well-understood topological properties. We again stress the impact of global twisting upon the ensuing knot types and unfoldings: such is the flavor of global bifurcation theory.

This work is supported by an NSF Graduate Research Fellowship (RG) and by AFOSR grant #91-0329 (PH). The authors would also like to thank F. J. Wicklin and Mike Sullivan for their useful comments.

Since completing this work, we have discovered the note by Turaev and Šilnikov [TS87], announcing results on unfoldings similar to and in agreement with Propositions 3, 4, and 5 of this work.

References

- [ABS82] V. Afraimovich, V. Bykov, and L. Silnikov. On structurally unstable attracting limit sets of Lorenz attractor type. *Trans. Moscow Math. Soc.*, 44:153–216, 1982.
- [BGKM91] C. Baesens, J. Guckenheimer, S. Kim, and R. S. MacKay. Three coupled oscillators: mode-locking, global bifurcations and toroidal chaos. *Physica D*, 49:387–475, 1991.
- [Bir75] J. S. Birman. *Braids, Links, and Mapping Class Groups*. Princeton University Press, Princeton, N.J., 1975.
- [Boy] P. Boyland. Braid types and a topological method for proving positive entropy. Preprint.
- [BW83a] J. Birman and R. F. Williams. Knotted periodic orbits in dynamical systems—I : Lorenz’s equations. *Topology*, 22(1):47–82, 1983.
- [BW83b] J. Birman and R. F. Williams. Knotted periodic orbits in dynamical systems—II : knot holders for fibered knots. *Cont. Math.*, 20:1–60, 1983.
- [CGT84] P. Coullet, P. Glendinning, and C. Tresser. Une nouvelle bifurcation de codimension 2: le collage de cycles. *C. R. Acad. Sc. Paris*, 299:253–256, 1984.
- [FW87] J. Franks and R. F. Williams. Braids and the Jones polynomial. *Trans. Am. Math. Soc.*, 303(1):97–108, 1987.
- [GGT84] J. Gambaudo, P. Glendinning, and C. Tresser. Collage de cycles et suites de Farey. *C. R. Acad. Sc. Paris*, 299:711–714, 1984.
- [GGT88] J. Gambaudo, P. Glendinning, and C. Tresser. The gluing bifurcation I: symbolic dynamics of the closed curves. *Nonlinearity*, 1:203–214, 1988.

- [GH83] J. Guckenheimer and P. J. Holmes. *Nonlinear Oscillations, Dynamical Systems, and Bifurcations of Vector Fields*. Springer-Verlag, New York, 1983.
- [GH93] R. Ghrist and P. Holmes. Knots and orbit genealogies in three dimensional flows. In *Bifurcations and Periodic Orbits of Vector Fields*, pages –. NATO ASI series, Kluwer Academic Press, 1993.
- [Gle88] P. Glendinning. Global bifurcation in flows. In T. Bedford and J. Swift, editors, *New Directions in Dynamical Systems*, pages 120–149. London Math. Society, Cambridge University Press, 1988.
- [GPTT] J. Gambaudo, I. Procaccia, S. Thomae, and C. Tresser. New universal scenarios for the onset of chaos in Lorenz-like flows. Preprint.
- [GT85] J. Gambaudo and C. Tresser. Dynamique régulière ou chaotique: applications du cercle ou de l'intervalle ayant une discontinuité. *C. R. Acad. Sc. Paris*, 300:311–313, 1985.
- [GT88] J. Gambaudo and C. Tresser. On the dynamics of quasi-contractions. *Bol. Soc. Brasil Math.*, 19:61–114, 1988.
- [GW79] J. Guckenheimer and R. F. Williams. Structural stability of Lorenz attractors. *Inst. Hautes Études Sci. Publ. Math.*, 50:59–72, 1979.
- [Hol86] P. J. Holmes. Knotted periodic orbits in suspensions of Smale's horseshoe: period multiplying and cabled knots. *Physica D*, 21:7–41, 1986.
- [Hol87] P. J. Holmes. Knotted periodic orbits in suspensions of annulus maps. *Proc. Roy. London Soc. A*, 411:351–378, 1987.
- [Hol88] P. J. Holmes. Knots and orbit genealogies in nonlinear oscillators. In T. Bedford and J. Swift, editors, *New Directions in Dynamical Systems*, pages 151–191. London Math. Society, Cambridge University Press, 1988.
- [Hol89] P. J. Holmes. Knotted periodic orbits in suspensions of Smale's horseshoe: extended families and bifurcation sequences. *Physica D*, 40:42–64, 1989.
- [HW85] P. J. Holmes and R. F. Williams. Knotted periodic orbits in suspensions of Smale's horseshoe: torus knots and bifurcation sequences. *Archive for Rational Mech. and Anal.*, 90(2):115–193, 1985.
- [Lor63] E. N. Lorenz. Deterministic non-periodic flow. *J. Atmospheric Sci.*, 20:130–141, 1963.
- [Mor78] J. Morgan. Nonsingular Morse-Smale flows on 3-dimensional manifolds. *Topology*, 18:41–54, 1978.
- [MP87] E. Meron and I. Procaccia. Gluing bifurcations in critical flows: the route to chaos in parametrically excited surface waves. *Phys. Rev. A*, 35 (9):4008–4011, 1987.
- [MSN⁺91] G. B. Mindlin, H. S. Solari, M. A. Natiello, R. Gilmore, and X. J. Hou. Topological analysis of chaotic time series data from the Belousov-Zhabotinskii reaction. *J. Nonlinear Sci.*, 1:147–173, 1991.
- [MT93a] F. A. McRobie and J. M. T. Thomson. Introduction to braids and knots in driven oscillators. To appear in *Int. J. Bifurcation and Chaos*, Preprint, April 1993.
- [MT93b] F. A. McRobie and J. M. T. Thomson. Knot types and bifurcation sequences of homoclinic and transient orbits of a single-degree-of-freedom driven oscillator. Submitted to *Dynamics and Stability of Systems*, Preprint, April 1993.
- [PTT87] I. Procaccia, S. Thomae, and C. Tresser. First-return maps as a unified renormalization scheme for dynamical systems. *Phys. Rev. A*, 35 (4):1884–1900, 1987.
- [Rol77] D. Rolfsen. *Knots and Links*. Publish or Perish, Berkely, CA, 1977.
- [TS87] D. Turaev and L. Silnikov. On bifurcations of a homoclinic 'figure eight' for a saddle with a negative saddle value. *Soviet Math. Dokl.*, 34:397–401, 1987.
- [Wad89] M. Wada. Closed orbits of nonsingular Morse-Smale flows on S^3 . *J. Math. Soc. Japan*, 41(3):405–413, 1989.
- [Zak93] M. Zaks. Scaling properties and renormalization invariants for the 'homoclinic quasiperiodicity'. *Physica D*, 62:300–316, 1993.